Oxidation of Metals, Vol. 58, Nos. 1/2, August 2002 (© 2002)

Effect of Cycle Frequency on High-Temperature Oxidation Behavior of Alumina-Forming Alloys

B. A. Pint,*,† P. F. Tortorelli,* and I. G. Wright*

Received November 29, 2000; revised February 7, 2002

Cycle frequency affects both high-temperature oxidation behavior and the method in which the cyclic test is conducted. Several issues are discussed using examples taken from results for Ni-base and Fe-base, alumina-forming alloys. For alloys that form adherent scales, cycle frequency has little effect on results over extended test times (≥500 hr). When an alloy forms a less adherent scale, reducing the cycle time often has the expected effect of increasing the mass loss per unit exposure time; however, the opposite effect is observed in other cases. Low-frequency cycle experiments can be conducted with specimens contained in alumina crucibles. This has the important benefit of collecting the spalled oxide and measuring the "total" mass gain, equivalent to the metal wastage. However, higher-frequency-cyclic tests cannot be performed with crucibles because of the large thermal mass and thermal-shock problems of alumina crucibles. The test method and cycle frequency ultimately have a strong effect on lifetime predictions.

KEY WORDS: alumina formers: cyclic testing; cycle frequency; testing method.

INTRODUCTION

Cyclic oxidation is one of the fundamental methods used to assess high-temperature environmental resistance of materials. During heating and cooling, the thermal expansion mismatch between metal and oxide results in thermal strains, which are often a primary cause of degradation to the protective external oxide scale.[1–4] The practical reason for this type of test is to simulate application cycles in a controlled manner. Ideally, the tests

*Oak Ridge National Laboratory, P.O. Box 2008, Oak Ridge, Tennessee 37831-6156.
†To whon all correspondence should be sent; e-mail: pintba@ornl.gov

0030-770X/02/0800-0000/0 © 2002 Plenum Publishing Corporation

should have a uniform heating rate, cooling rate, and cycle duration. While the cyclic test should be designed to mimic the expected duty cycle, it is attractive to use standardized tests that allow direct performance comparisons of different materials and provide valuable information for the understanding of cracking and spallation mechanisms.[5–11]

One important variable in cyclic oxidation testing is the cycle frequency or its inverse—the length of time at temperature for each cycle. Surprisingly, this variable is rarely discussed in any detail.[12–14] Longer cycle times are of importance to projects such as the U.S. Department of Energy's Advanced Turbine Systems Program, which is attempting to transfer state-of-the-art materials technology from aircraft engines to land-based, gas turbine engines for power generation.[15,16] However, the duty cycle for aircraft is much shorter than that for base-load power generation. Consequently, there has been concern that materials and, in particular, coatings which are well-suited for aircraft applications will perform differently in the longer-term cycles experienced in land-based gas turbines, heat exchangers, or other power-generation technologies.

A second aspect of cycle frequency relates to data collection for lifetime predictions. If more oxidation-resistant alloys (which are generally more expensive) are to be implemented in commercial applications, it is essential to clearly define the expected benefit in life extension that these materials are expected to achieve. Depending on the cycle frequency and the procedures used in conducting the experiment, very different lifetime predictions can result. Therefore, it is essential to correctly select appropriate test conditions and methods for collecting data in order to develop a reliable prediction.

This paper considers a wide range of experimental data from alumina-forming alloys in order to illustrate some basic issues regarding cycle frequency effects and test procedures. Additional data are provided beyond that previously presented,[17] and the focus is mainly on mass change data. A subsequent paper will provide information on the effect of cycle frequency on scale microstructure.[18] Two forms of testing are discussed: uncontained cycling, which is more appropriate for high-frequency tests, and contained cycling, where the specimen is held in an individual alumina crucible, which collects spalled and/or evaporated oxide. It is demonstrated that, for lifetime predictions, the total mass-gain data from contained cycling is more useful than the specimen mass-change data alone. However, contained cycling tests are more labor and equipment intensive and are not appropriate for high cycle frequencies and certain exposure conditions.

EXPERIMENTAL PROCEDURE

A variety of alloys were used in this study. Chemical compositions of Ni-base superalloys,[19] NiAl variations,[20] Pt-containing alloys,[21] Fe-base

castings,[22,23] ODS FeCrAl[24–26] and ODS Fe_3Al[26,27] are given in detail elsewhere. Unless otherwise specified, specimens were polished to a 0.3 μm finish and ultrasonically cleaned in acetone and methanol prior to oxidation.

Short-term (1–10 hr,) high-frequency cycle tests were performed in a computer-controlled cyclic rig in dry flowing O_2, with seven uncontained specimens hanging, connected by Pt–Rh wires to individual alumina rods, in a vertical furnace. The cooling time between cycles was 10 min when specimen temperatures reached approximately 25°C. Long-term (100–500 hr), low-frequency cycle tests were conducted in box or horizontal tube furnaces in laboratory air with the specimen contained in a preannealed alumina crucible with an alumina lid. Specimens were cooled for at least 24 hr prior to weighing. Specimens were weighed on a Mettler model AG245 balance. Isothermal kinetics were measured using a Cahn model 1000 microbalance.

This paper focuses on gravimetric results as the principal indicator of the influence of cycle frequency on performance. Although limited microstructural information is provided, some conclusions are based on characterizations by metallography, X-ray diffraction (XRD), scanning-electron microscopy (SEM), energy-dispersive X-ray spectroscopy (EDS), and transmission-electron microscopy (TEM). More characterization data will be provided in a subsequent paper.[18]

RESULTS

The experimental results are divided by alloy type in order to demonstrate several important points about the role of cycle frequency on oxidation behavior.

Ni–Base Superalloys: Sulfur Effects

A series of modifications of General Electric Aircraft Engines' alloy René N5, a single-crystal Ni-base superalloy, were cast in order to investigate the role of Y and S on their oxidation performance.[19] Castings without Y were desulfurized both in the melt (N5B, N5C, and N5D) and by hydrogen annealing (N5AH). While it has been widely observed that desulfurization improves performance in high-frequency cycles,[28–33] less low-frequency cyclic testing has been performed.[19]

The specimen mass-change data at 1100°C using three different cycle times are shown in Fig. 1. Hafnium-doped NiAl is included in the figures as a reference. The 1- and 10-hr cycles were conducted in an uncontained test while the 100-hr cycles were conducted using alumina crucibles. Also, the 10-hr specimens were only polished to 600-grit SiC finish. A variety of alloys illustrate that both hydrogen annealing and melt desulfurization

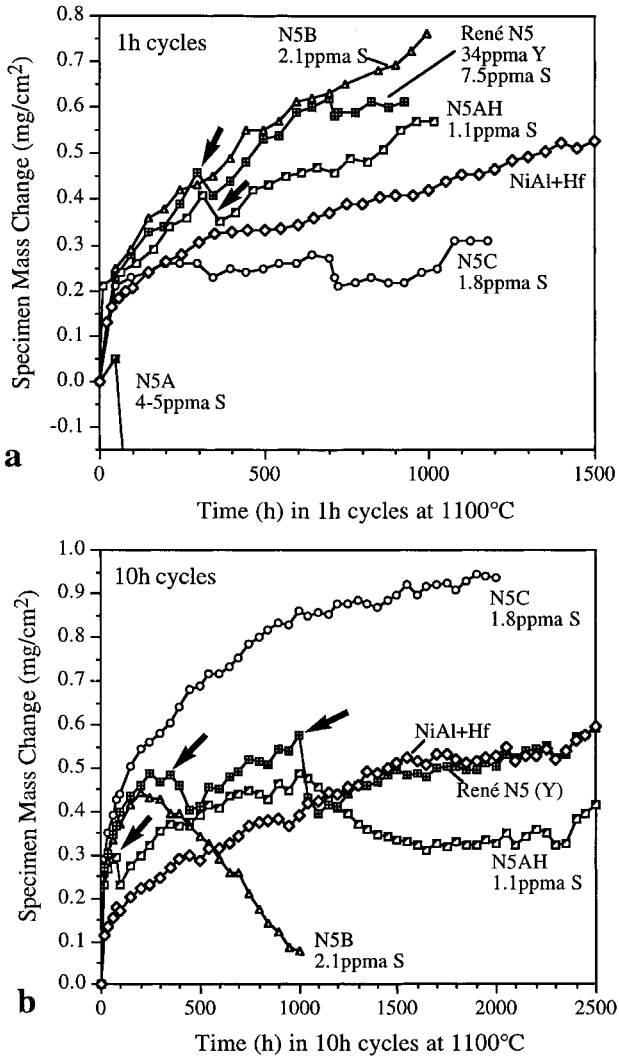

Fig. 1. Specimen mass gain for several single-crystal Ni-base superalloys oxidized at 1100°C using (a) 1-, (b) 10-, and (c) 100-hr cycles. Removing indigenous sulfur in the melt or by hydrogen annealing improved scale adhesion, but not always to the same degree. Alloy N5B with 2.1 ppma S did not lose mass in 1-hr cycles, but did in 10- and 100-hr cycles. In shorter cycles (a) and (b), arrows mark specimen losses not followed by continued mass loss. These events are linked to spallation of the transient Ni-rich outer scale and not to spallation of the alumina scale.

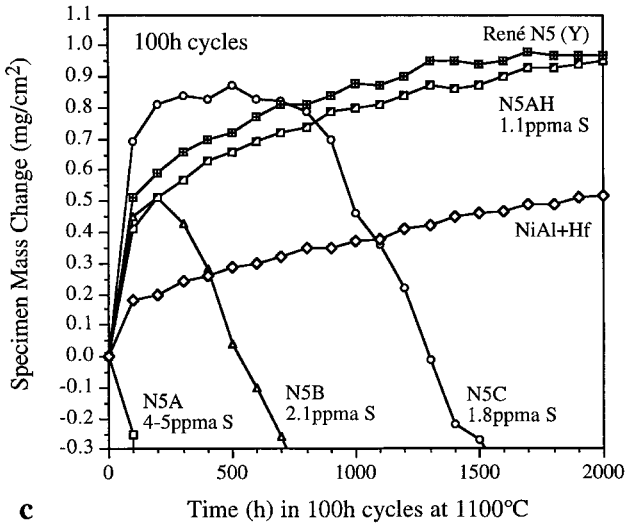

Fig. 1. Continued.

result in an improvement in scale adhesion relative to a Y-free, nominal sulfur content (4–5 ppma) casting (N5A). However, the desulfurized alloys differentiated somewhat in the various tests. In particular, N5B (melt desulfurized, 2.1 ppma S) showed little spallation in 1-hr cycles but showed progressively higher mass losses with increasing cycle time (Fig. 2a). Increasing the cycle time to 100 hr also resulted in significant spallation for N5C (melt desulfurized, 1.8 ppma S). The time to onset of spallation in 100-hr cycles increased with decreasing sulfur (Fig. 1c). In 100-hr cycles, the standard N5 (with Y) and N5AH both accumulated 3000 hr of exposure time with only minor spallation. However, after 1500 hr in 10-hr cycles, N5AH showed steady mass losses while N5 did not show the same downward trend.

When the mass losses were significant, it was clear from examination of the specimens that spallation occurred at the metal interface.[19] However, some spallation appeared to only include the outer transient scale, which, because of its blue color, was easy to observe. In both 1- and 10-hr cycles, occasional minor, but distinct, drops in mass were measured (arrows in Figs. 1a and 1b) followed by mass gains. This was most evident for the castings with more adherent scales, N5 and N5AH, but not for NiAl + Hf (Fig. 2a), which does not form a Ni-rich transient oxide. Note that this resulted in noticeably lower mass gains for specimens cycled for 1- and 10-hr cycles compared to 100 hr (Fig. 2b). These drops were attributed to the spallation of the transient, spineltype scale [e.g., Fig. 3, typically $(Ni, Co)(Al, Cr)_2O_4$],

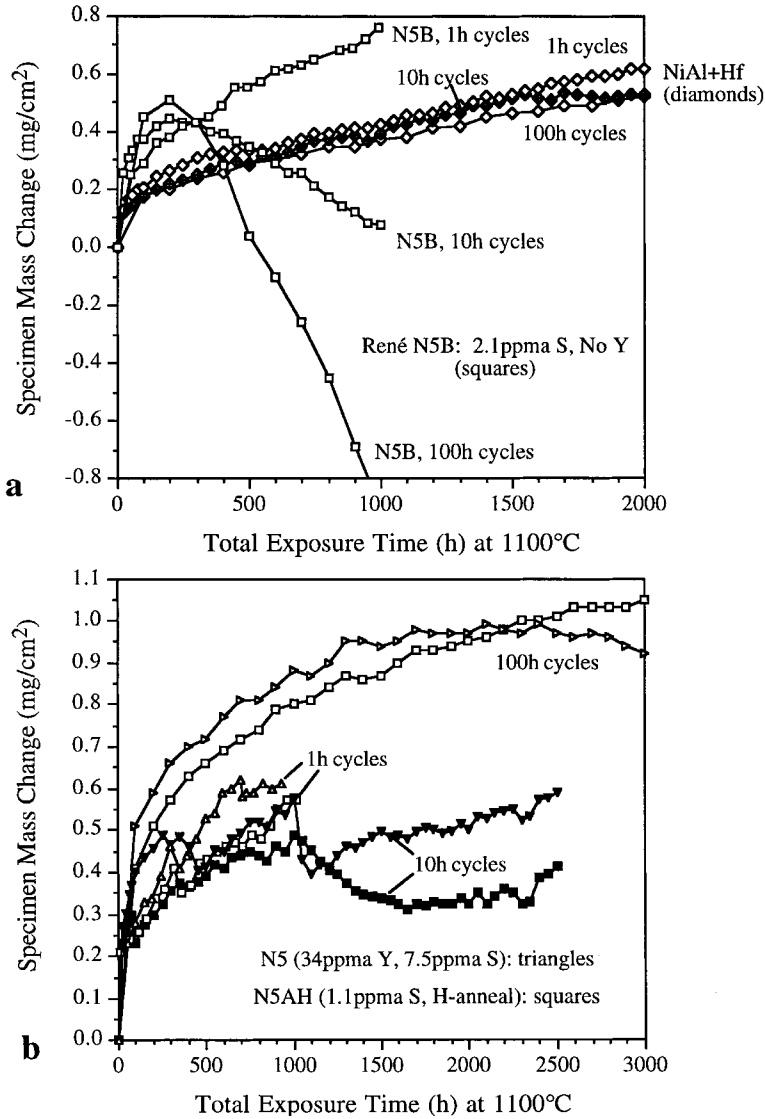

Fig. 2. Specimen mass gain for various cycle times at 1100°C for (a) N5B and NiAl + Hf and (b) standard N5 (with Y) and hydrogen annealed N5, N5AH. Increased cycle frequency decreased scale spallation on N5B, but had little effect on NiAl + Hf. The lower mass gains in shorter time cycles for N5 and N5AH likely reflects spallation of the transient oxide. In 100-hr cycles, N5 and N5AH still show little spallation.

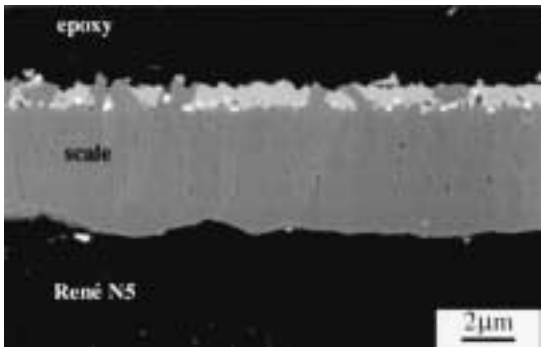

Fig. 3. SEM backscattered electron image of a polished cross section of scale formed on N5 after 100 hr at 1200°C. The transient scale formed at the gas–side interface contains predominantly Ni, Co, and Cr and the very bright particles are rich in Ta as determined by EDS analysis (see Ref. 34).

which can spall and still leave behind the underlying, rate-limiting, alumina layer.

These relatively small deviations in specimen mass change make performance comparisons difficult among alloys that do not exhibit large amounts of spallation. One way to try to resolve these differences is to calculate rate constants from the various specimen masses, k_{ps} (Table I). These values can be compared to those from isothermal thermogravimetric

Table I. Parabolic Rate Constants, g^2/cm^4 sec ($\times 10^{-14}$) at 1100°C for Variations of René N5, a Single Crystal Ni-Base Superalloy, for Different Cycle Times and Isothermally

		Calculated from specimen ΔM (k_{ps})			Total ΔM (k_{pt})	Isothermal ΔM (k_{pi})
Alloy	Comments	1 hr	10 hr	100 hr[a]	100 hr	100 hr
β-NiAl + Hf	Cast, 0.05 at.% Hf	4.5	3.3	2.9 (6)	2.7	11.4
N5	Standard 34 ppma Y, 1.1 ppma S	10.4	7.1	6.8 (42)	14.1	31.6
N5A	No Y 5.5 ppma S	—	—	—	11,800	132
N5B	Melt-desulfurized No Y, 2.1 ppma S	13.1	—	(40)	64.5	44.7
N5C	Melt-desulfurized No Y, 1.8 ppma S	—	13.6	(72)	58.5	62.1
N5AH	H_2-annealed No Y, 1.1 ppma S	5.9	3.2	4.9 (32)	5.9	35.7

[a]Values in parenthesis estimated from first 200–300 hr data.

tests,[19] k_{pi}, and to a rate constant calculated from the total mass gain measured for the 100-hr cycles, k_{pt}. In general, the substrates which formed more adherent scales (N5, N5AH) exhibited lower rate constants (by a factor of four to ten compared to N5B and N5C) suggesting that there may be less transient scale formation or a reactive-element (RE) effect[35–37] on the scale growth rate. While the low-S alloys do not contain Y, they do contain Hf, which has been shown to have a dramatic effect on the scale growth rate in β-NiAl.[20,21] It also may be important that H_2 annealing removed C as well as S from the superalloy,[19] which may affect the Hf activity in the substrate.[33] Recent work has shown a degradation in scale adhesion on NiAl + Hf when the C content was increased.[38] Also, higher isothermal rates for N5B and N5C indicate that a thicker alumina scale formed. A thicker oxide scale would have higher strains on cooling than a thinner scale formed on an alloy with a slower scale-growth rate.

While there is some benefit associated with comparing these types of calculated rate constants (Table I), they only provide qualitative information about relative rates of spallation and are not well suited to incorporation into a quantitative spallation model. One difficulty in comparing these rates is that the isothermal experiments were run for 100–200 hr while the cyclic experiments generally were of ≥1000 hr duration. This type of comparison requires a large extrapolation or much longer isothermal tests. Because $k_{pi} > k_{pt}$ for the substrates with the most adherent scales, the scale growth rate decreases with time and possibly is affected by the transient scale formation.

NiAl

When properly doped with a RE such as Zr or Hf, NiAl is one of the most oxidation-resistant alloys. This is clearly illustrated in Fig. 2a, where NiAl + Hf is observed to show very similar mass gains up to 1000 hr, independent of cycle frequency. The mass gains were extremely low because of the optimal Hf doping, which has been found to reduce the parabolic rate constant by a factor of ten or more at this temperature.[20,21] It is likely that these curves for different cycle frequencies would differentiate, but only after much longer total exposure times.

In order to accelerate the oxidation testing by forming a thicker scale, the same types of exposures were performed at 1200°C (Fig. 4). At the higher temperature, the mass changes also were low relative to other alumina formers, but some differentiation occurred, which was attributed to the quality of the casting. Since NiAl is a brittle material, small casting cracks are often unavoidable. However, these small (<5 mm) defects can alter the mass gain significantly. Figure 4 shows two different NiAl + Hf

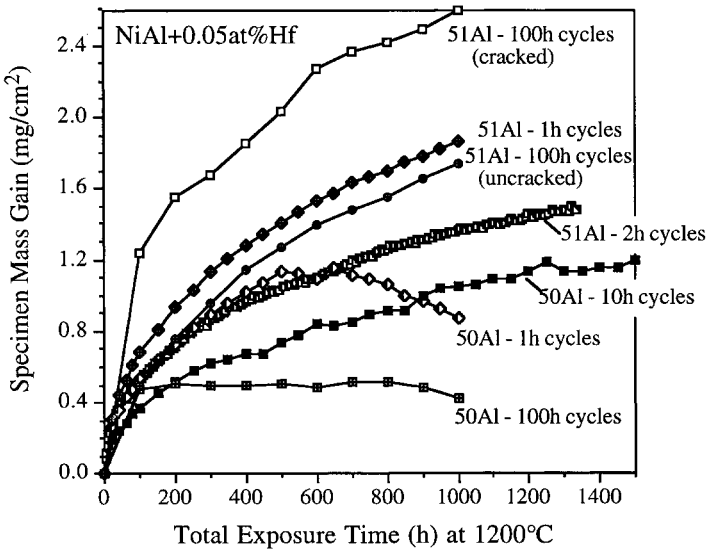

Fig. 4. Specimen mass gain for NiAl + 0.05 at.%Hf for various cycle times at 1200°C. For the slow-growing and very adherent alumina scale formed on Hf-doped NiAl, the effect of casting composition and quality was as important as cycle frequency. For casting #1, much longer times will be required to determine the effect of cycle frequency. In 100-hr cycles, a higher mass gain was noted when the specimen contained several cracks.

castings with the same 0.05 at.% Hf, <4 ppma S, 0.04 at.% C contents, but slightly different Al contents, 51.0 at.%Al in one and 50.1 at.%Al in the other. Somewhat higher mass gains with less visible scale spallation was noted for the casting with 51%Al. However, specimens with visible cracks showed a significantly higher mass gain in 100-hr cycles and a slightly lower mass gain in 2-hr cycles. The higher mass gain was attributed to oxide formation in the cracks, which made them appear white, and the lower mass gain to increased spallation near the cracks, when the cycle frequency was higher. The casting with 50 at.%Al generally showed more scale spallation. This difference could be attributed to the lower Al content, but subsequent work has shown that casting quality and the Hf/C ratio are likely to be more important factors. While not observed in this case, hyperstoichiometric NiAl castings generally are more defective because they are more brittle than hypostoichiometric castings. Composition effects are still being considered, but the effects are minor and difficult to separate. It is important to recognize that even a "defective" NiAl + Hf specimen performs better than most other alumina formers in terms of resistance to scale spallation.

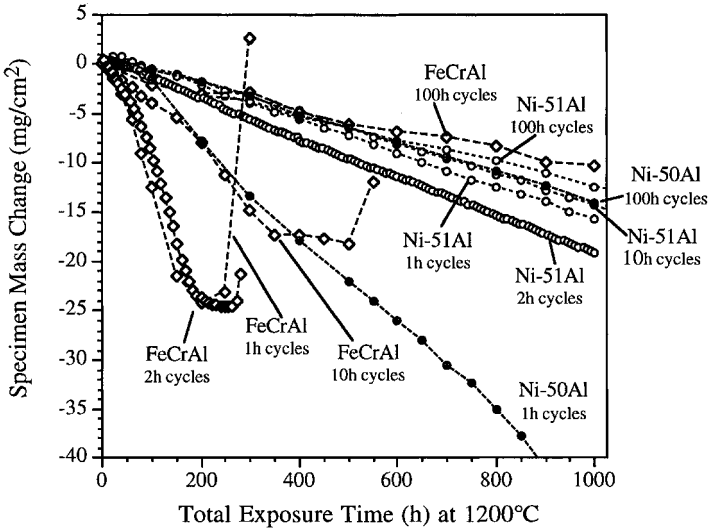

Fig. 5. Specimen mass gain for undoped FeCrAl and undoped NiAl as a function of cycle time at 1200°C. In 100-hr cycles, all alloys behaved similarly with an alumina scale forming and spalling after each cycle. In 1-hr cycles, spallation was more severe for FeCrAl, but there was wide variability for two different near-stoichiometry NiAl alloys. Curves for FeCrAl, end at breakaway for 1-, 2-, and 10-hr cycles. For Ni–51Al, cycle frequency had little effect on spallation rate.

The role of cycle frequency also was evaluated on undoped NiAl (Fig. 5). On one casting (50.2 at.% Al, 27 ppma S), switching from 100- to 1-hr cycles caused a significant increase in the linear rate of mass loss. After 1000, 1-hr cycles, the specimen had cracked and was forming large amounts of Ni-rich oxide and spinel. A second casting (51.2 at.%Al, 3 ppma S), showed only a slight increase in the linear spallation rates when the cyclic time was decreased from 100 to 1 hr. Again, the difference in performance between the two castings could be an effect of Al, S, or C contents or casting defects. However, it is surprising that the two castings showed identical performance in 100-hr cycles, but increasing the cyclic frequency showed a significant effect only on the performance of Ni–50.2%Al. This suggests that the composition effects become more important with a higher cyclic frequency.

Pt-Containing Alloys

To study the role of Pt in aluminides, a series of Pt-containing alloys was cast. Previous papers have reported that cast (Ni, Pt)Al and PtAl alloys showed little spallation in 1-hr cyclic testing up to 500 hr at 1150°C and

100 hr at 1200°C.[21,39] Alloys with a Pt addition showed a considerable improvement in spallation resistance over cast, undoped NiAl, but not as good as that observed for Hf-doped NiAl (Fig. 4). However, in 100-hr cyclic tests at a lower temperature (1100°C) there was little improvement in the total mass gain associated with PtAl or Pt-doped NiAl (2.3 at.%,10 wt.%Pt) (Fig. 6). A lower total mass gain was observed for a casting with 50.2 at.%Al (4 ppma S) compared to one with 51.8 at.%Al (10 ppma S). The alloy with the higher Al content was much more brittle and the casting with the lower Al content contained fewer defects. Nevertheless, the specimen mass changes (dashed lines) show that NiPt–50Al underwent significant scale spallation after 20, 100-hr cycles. Undoped NiAl (50.1 at.%Al, < 4 ppma S) and NiPt–52Al showed a nearly linear mass gain increase after the first 500 hr, indicating a large amount of spallation after each cycle. The PtAl casting showed slightly less spallation than NiAl or (Ni, Pt)Al. However, this reduction in specimen mass loss was mainly a result of cracking and internal oxidation of PtAl[39] and not due to a more adherent alumina scale.

Total mass gains were similar for NiAl, PtAl, (Ni, Pt)–50Al and (Ni, Pt)–52Al at 1200°C after 10, 100-hr cycles. However, this is not surprising, as the beneficial effect of Pt was only observed for 100, 1-hr cycles at this temperature, which is the equivalent of only one 100 hr cycle.

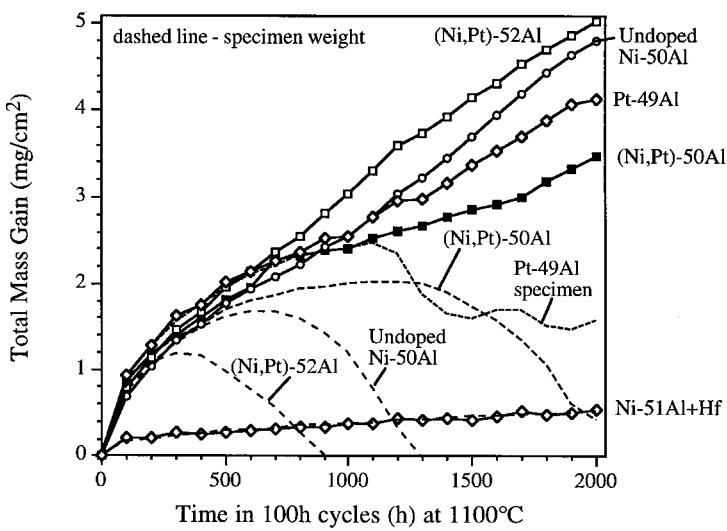

Fig. 6. Specimen (dashed line) and total mass gains (symbols) for several aluminides during 100-hr cycles in crucibles at 1100°C in air. A beneficial effect of Pt was not observed when the cycle time was increased to 100 hr; however, Hf-doped NiAl showed no spallation.

Cyclic testing also was performed at 1100°C on a NiPt–49.6 at.%Al casting with 5.2 at.% (20 wt.%) Pt, which contains a higher Pt content to reflect that generally observed in Pt-modified aluminide coatings on commercial Ni-base superalloys.[40,41] A slightly higher specimen mass gain was observed in 100-hr cycles compared to 1-hr cycles (Fig. 7), but the higher total mass gain in 100-hr cycles indicates that some scale spallation was occurring. Three specimens which were stopped at 500 hr for microstructural characterization[18] showed almost identical mass gains in 1-, 10- and 100-hr cycles.

Similar to N5B above, Pt-containing aluminides also showed significant spallation in 100-hr cycles at 1100°C, an inverse effect of cycle frequency, with spallation increasing as frequency decreased. If the role of Pt is to slow the growth of interfacial voids,[39] this may explain the negative effect of longer cycle time. With a low-cycle frequency, the extended time at temperature allows for larger voids to grow at the metal–scale interface.[42,43] Smaller voids formed during shorter cycles may limit the damage to the scale and allow a healing alumina layer to quickly form, whereas large voids may

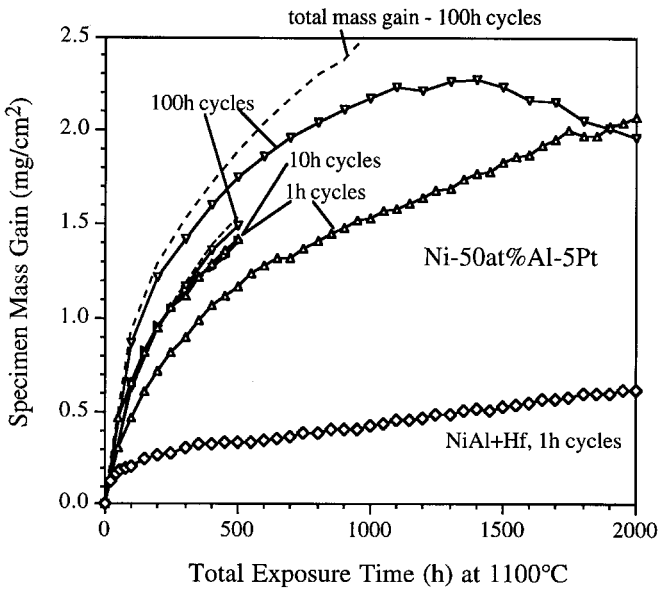

Fig. 7. Specimen mass gain and the total mass gain during 100-hr cycles (dashed line) for 1.5-mm thick Ni–50 at.%Al–5%Pt as a function of cycle time at 1100°C. Similar mass gains were noted in 1-, 10-, and 100-hr cycles, although the mass gains were somewhat higher in 100-hr cycles.

result in major scale losses. This result is of particular concern for Pt-modified aluminide coatings being considered for land-based gas turbine engines. For this long-cycle application, the benefit of Pt additions may be substantially reduced.

FeCrAl-Base Alloys

A somewhat different response to cycling has been observed for iron-base alloys compared to Ni-base alloys. For undoped FeCrAl (20.1 at.%Cr, 9.6%Al, 85 ppma S) in 100-hr cycles, the performance was nearly identical to Ni–50Al and Ni–51Al (Fig. 5). This was not surprising as the scale-growth rate is similar on both alloys,[37] and essentially all of the oxide spalls after each cycle. However, when the cyclic frequency was increased, the mass loss of undoped FeCrAl increased significantly and breakaway oxidation (i.e., FeO_x formation) occurred after 550 hr in 10-hr cycles, 280 hr in 2-hr cycles, and 300 hr in 1-hr cycles. (The specimens were 1.5 mm ± 5% in thickness to make this comparison realistic.) The lower Al content of FeCrAl relative to NiAl is a major reason for the different behavior of FeCrAl. Particularly with high-cycle frequency, scale spallation from FeCrAl quickly leads to Al depletion and the formation of Fe-rich spinel, followed by the formation of iron oxide. These reaction products increase the rate of oxide growth and thus higher rates of spallation. The increasing mass losses of FeCrAl with increasing cycle frequency is the more expected result.

When doped with Y, FeCrAl forms a much more adherent alumina scale.[44,45] As a result, little effect of cycle frequency was observed up to ≈500 hr at 1200°C (Fig. 8). After a total exposure of 5000 hr in 100-hr cycles, the specimen exhibited virtually no spalled oxide and only a few macrocracks in the oxide. During testing in 1-hr cycles, the scale began to crack and deform much earlier with an associated continuous mass loss, but did not go into breakaway oxidation until 8800, 1-hr cycles. In both cases, the specimen thickness was ≈1.5 mm. In 10-hr cycle testing, only minor spallation was observed after 2000 hr and a specimen exposed for 2-hr cycles also began to spall after ≈700 hr of total exposure.

In order to improve high-temperature strength as well as oxidation performance, Y-containing oxide dispersions are often added to FeCrAl. The effect of cycle frequency on one such alloy, Plansee alloy PM2000, is shown in Fig. 9. This alloy showed some important differences compared to FeCrAlY. In 1-hr cycles, the scale spallation started later (≈900 cycles), but was more severe, with a final specimen life of 3950 cycles for a 1.7 mm thick specimen. Comparing the results from 10- and 100-hr cycle tests, the specimen mass changes were almost identical after 2000 hr. However, the

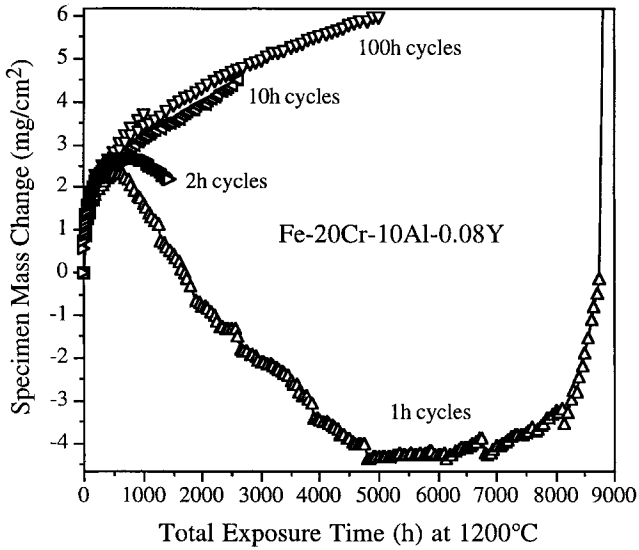

Fig. 8. Specimen mass gain for 1.5-mm thick FeCrAlY as a function of cycle time at 1200°C. For the very adherent alumina scale formed on FeCrAlY, 600 hr was required to begin differentiation between 1- and 100-hr cycles. After 5000 hr in 100-hr cycles, virtually no scale spallation was observed.

difference between the specimen and total mass gains during 100-hr cycles indicated some spallation was occurring after 2000 hr, but it was concentrated at the specimen edges. After 5000 hr in 100-hr cycles, spallation was observed on the specimen faces as well. Thus, this alloy showed more spallation and a shorter life in oxidation testing than FeCrAlY. The important factors are likely the higher strength of the PM2000 substrate, which is less likely to relieve stress,[10,11] and the formation of oxide pegs due to internal oxidation of Y in FeCrAlY,[44–47] which does not occur with oxide-dispersed PM2000. Further discussion of these differences is beyond the scope of this paper.

A final example of a cycle-frequency effect is Yb_2O_3-dispersed FeCrAl (0.2 at.%Yb) (Fig. 10). This composition is overdoped with Yb[24,25] and thus accelerated scale growth occurs resulting in reduced times to breakaway oxidation (rapid mass gain associated with the formation of FeO_x). While it is widely recognized that too much RE dopant can have negative effects, there is no mechanism to explain this problem. Elements such as La, Ce, Hf, Yb, and Zr are susceptible to overdoping problems. In this particular case, the scale grows much faster than normal, but is somewhat adherent

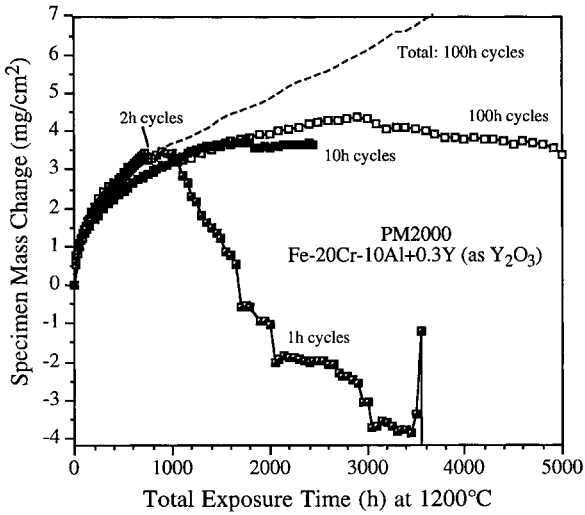

Fig. 9. Specimen mass gain and the total mass gain during 100-hr cycles (dashed line) for a commercial FeCrAl + Y_2O_3 alloy, PM2000, as a function of cycle time at 1200°C. Little difference was observed between 10- and 100-hr cycles, but significant mass losses were observed for 1-hr cycles. The difference between the total and specimen mass gains during 100-hr cycles indicates scale spallation.

(compare total and specimen mass losses during 100-hr cycles) resulting in mass gains rather than mass losses typical of nonprotective scales. It is noted that higher cycle frequencies resulted in shorter lifetimes. Although the scale did not spall significantly, it was not protective (as has been described elsewhere[48]) and, therefore, increasing the cycle frequency reduced the time to breakaway oxidation.

Fe_3Al-Base Alloys

For iron aluminides, the performance is somewhat different. Three examples are given: cast alloys with Zr (FAL: Fe–28Al–5Cr–0.1Zr) and Hf (FAS + Hf: Fe–28Al–2Cr–0.05Hf) and an oxide-dispersion strengthened substrate, PMFAS: Fe–27Al–2 Cr–0.2Y (as Y_2O_3) (Figs. 11–13, respectively). Several papers have pointed out the increased scale spallation for iron aluminides compared to RE-doped FeCrAl or NiAl.[22–24,26,27] [This difference is attributed to the significantly higher coefficient of thermal expansion (CTE) of Fe_3Al.][23,26] Of the three alloys, Hf-doped iron aluminide showed the best results. For example, it has the longest lifetime in 1-hr

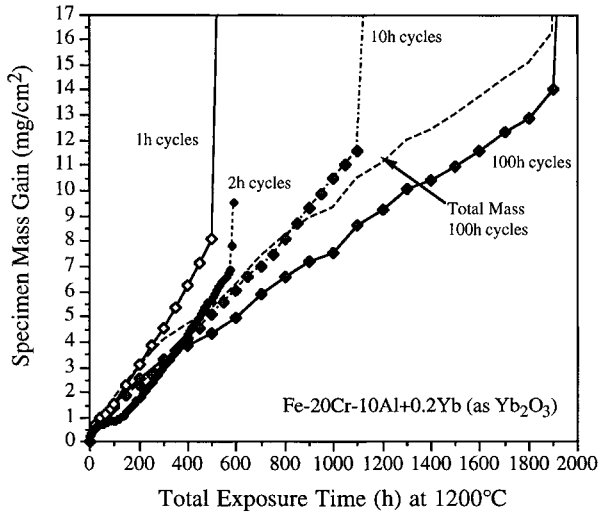

Fig. 10. Specimen mass gain and the total mass gain during 100-hr cycles (dashed line) for 1.5-mm thick FeCrAl + Yb_2O_3 as a function of cycle time at 1200°C. The addition of 0.2 at.%Yb resulted in rapid scale growth and relatively short lifetimes. The constant increases indicate a scale that did not spall but was not protective.

cycles and the lowest total mass gain after 50, 100-hr cycles at 1200°C (Fig. 12). This difference is attributed to the slower growing scale (similar to that for Hf-doped NiAl) for the scale on FAS + Hf.[23] However, the CTE-related scale-spallation problem was not corrected by Hf doping; thus, this alloy performs much worse than Hf-doped NiAl (Fig. 4).

For each of the three alloys, increasing the cycle frequency initially resulted in more scale spallation. However, unlike Ni-base alloys, the mass loss did not continue linearly. This was observed in 1-hr cycles for FAL and FAS + Hf and, in most cases, for PMFAS. The nonlinear specimen mass loss is associated with several different phenomena, represented by four different stages in the specimen mass change curve. A schematic example for Fe-base alloys is given in Fig. 14. The first two stages and last stage also are common to Ni-base alloys: an adherent (mass gain) stage followed by linear spallation (mass loss) and finishing with rapid mass gain of breakaway oxidation. For Fe-base alloys, however, the rate of mass loss often decreases to nearly zero when the alloy begins to form spinel oxide and usually starts to deform. The deformation effect is reflected in the mass-loss data for FAL (Fig. 11). When a thinner (1-mm) specimen was used, the

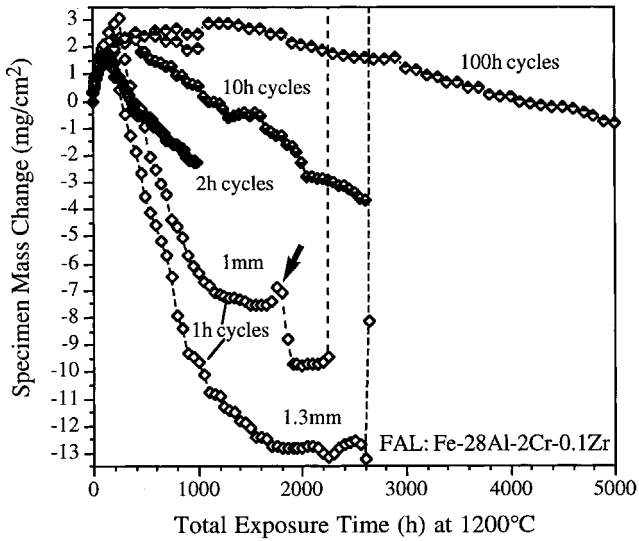

Fig. 11. Specimen mass gain for cast/extruded Fe–28Al–2Cr–0.1Zr as a function of cycle time at 1200C. After 200 hr, higher cycle frequency resulted in a significant increase in the amount of specimen mass loss. This behavior also was affected by specimen thickness. At one point (arrow), the specimen appeared to begin breakaway oxidation, but the affected area broke off and the specimen continued for several hundred hours.

onset of specimen deformation (≈1000 hr) was earlier and the mass loss began to level off sooner. A thicker specimen (1.3 mm) continued to lose mass after 1700 hr, although the rate of loss had decreased. For a 1.7 mm thick FAS + Hf specimen, alternating mass gains and mass losses began after 3000, 1-hr cycles. For 1.5 mm thick PMFAS specimens, mass loss was arrested for 100-hr cycles at 2000 hr, 10-hr cycles at 1300 hr, and 1-hr cycles at 800 hr (Fig. 13). In each case, the specimen deformed and began forming Fe-rich spinel when the mass began to increase.

Thus, unlike most results for Ni-base alloys (e.g., NiAl and NiCrAl), specimen mass losses due to thermal cycling are less well-behaved for Fe-base alloys. This problem is illustrated in Fig. 15 for several commercial and ORNL-produced ODS FeCrAl alloys with a nominal 1.5-mm specimen thickness. If the data are examined after only 1000 hr (vertical dashed line), it is difficult to use this information to accurately predict the long-term performance of the different materials. The commercial Kanthal alloy APM and Plansee alloy PM2000 appear to be performing similarly and yet their subsequent behavior is radically different. After 1000 hr, both show less

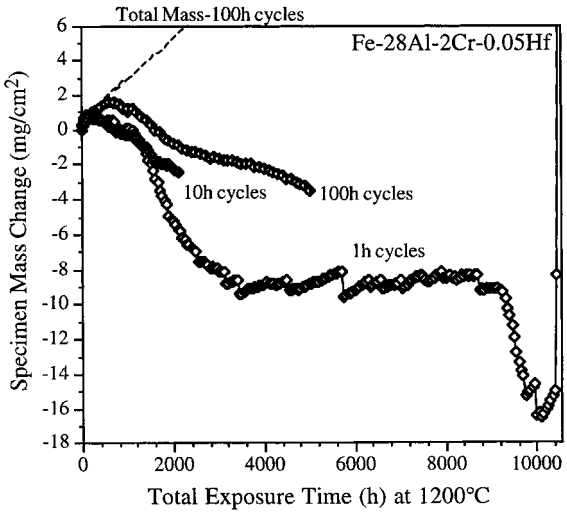

Fig. 12. Specimen mass gain and the total mass gain during 100-hr cycles (dashed line) for Fe–28Al–2Cr + Hf as a function of cycle time at 1200°C. The addition of Hf resulted in better performance compared to Zr-doped Fe_3Al. The addition of Hf did not strongly improve the scale adhesion, but did reduce the scale growth rate.

scale spallation than FeCrAlY and yet neither can match the ultimate life of FeCrAlY (Table II). Likewise, FeCrAl codoped with Y_2O_3 and Ta_2O_5 initially appears to be performing very poorly because of the large amount of spallation; yet, it has a similar life as Y_2O_3-dispersed FeCrAl and FeCrAl codoped with Y_2O_3 and TiO_2. There is little indication that FeCrAl codoped with Y_2O_3 and CaO will have a life nearly double the others. It also has been suggested to use the time to zero mass change as a measure of performance for modeling lifetime.[14] Again, this may be applicable to Ni-base alloys but, for these materials, the time to zero mass change in Fig. 15 gives no indication of time to breakaway. Several materials, including Kanthal alloy APM, never return to zero mass change. With no general pattern for the various specimens, it is difficult to see how specimen mass-change data alone could be used in a lifetime prediction model for Fe-base alumina formers. As a result, the only important number generated by this type of experiment is the time to breakaway (Table II), which, for the best alloys, is much longer than 2000, 1-hr cycles and, therefore, involves a large amount of experimental time.

An alternative way to collect similar data is to use a contained-cyclic test, which yields both specimen and total mass gain (Figs. 16 and 17).

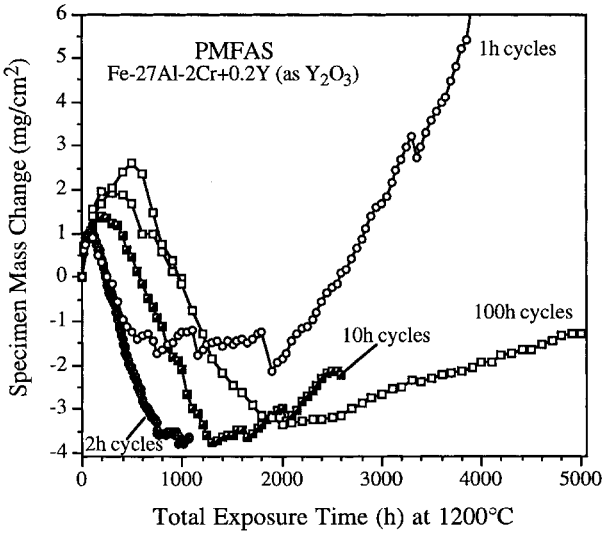

Fig. 13. Specimen mass gain for 1.5 mm thick ODS Fe_3Al as a function of cycle time at 1200°C. Initially, a lower cycle frequency resulted in less specimen mass loss with time. In 1-hr cycles, mass loss was arrested when the specimen began to deform and form spinel.

The specimen mass change is also obtained (dashed lines), but, whereas the specimen masses follow different patterns, the total mass gains are reasonably well-behaved. Because the total mass gain is easily correlated with metal wastage (or Al consumption), it is much more useful in calculating lifetimes.[22,49–52]

When all the uniformly collected data are placed together, it is easier to evaluate the relative performance of various alloys. For instance, at 1200°C, ODS Fe_3Al showed a higher mass gain than FeCrAl-based alloys, but performed better than $Fe_3Al + Zr$. At 1100°C (Fig. 16), FeCrAlY began with higher mass gains than PM2000 because of internal oxidation of Y.[45–47] However, because of scale spallation in the long term, PM2000 either showed similar mass gains (1100°C) or higher mass gains (1200°C). Finally, it is clear that the scale on Hf-doped NiAl grows substantially slower than other alloys, which also form adherent scales (Fig. 16).

DISCUSSION

While cycle frequency has a significant effect on oxidation performance, it is rarely discussed in the oxidation literature.[12–14,17] It was shown

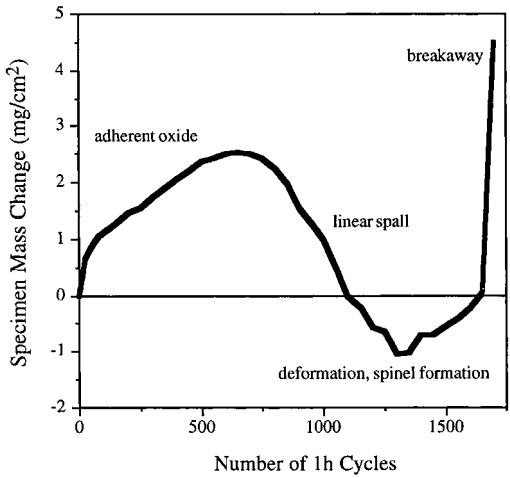

Fig. 14. Representative example of specimen mass change for Fe-base alumina-forming alloys in 1-hr cycles at 1200°C. Behavior tends to follow four periods: (1) adherent oxide formation, i.e., no spallation with mass gains comparable to those measured isothermally; (2) onset of spallation, sometimes following a linear loss, like that observed for Ni-base alloys; (3) substrate deformation (warping or curving) usually accompanied by spinel formation and specimen no longer losing mass and, finally, gaining weight prior to (4) breakaway oxidation, i.e the formation of FeO.

above that the effects of cycle frequency were not consistent among alloy systems. In some cases, higher cycle frequencies (shorter cycles) increased oxidation wastage, while in others, the opposite effect was observed. There are two broad competing factors when cycle frequency is decreased: (1) Because the frequency of thermal stresses decreases, scales containing defects capable of concentrating the stresses generated in each cooling cycle or causing fracture are subjected to fewer thermal-stress events. Any defects nucleated by thermal cycling would also accumulate at a slower rate. (2) Because scales and any defects developed at temperature (such as interfacial voids) have additional time to increase in size between thermal stresses, a larger strain must be accommodated in the cooling cycle and larger defects may increase the amount of spallation. Thus, increasing the cycle frequency could yield a positive [e.g., N5B and (Ni, Pt)Al] or negative (e.g., Ni–50Al, FeCrAl, FeCrAlY, iron aluminides) effect on the rate of spallation and empirically, both negative and positive effects have been observed. The more expected result is that higher cycle frequency should cause far more damage to the scale than low-frequency cycles.

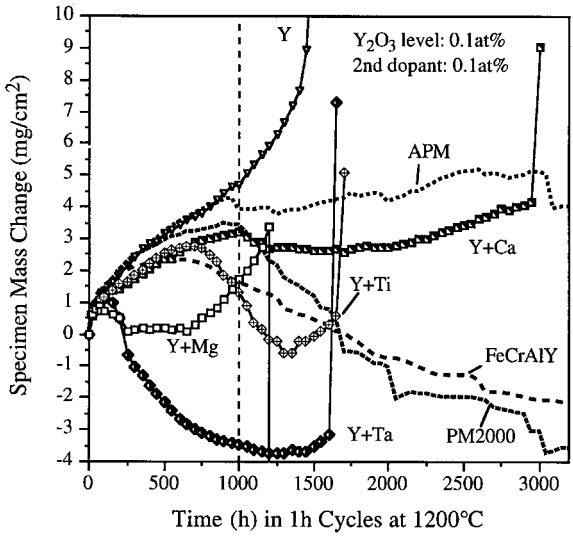

Fig. 15. Specimen mass gain for ≈1.5-mm thick FeCrAl alloys in 1-hr cycles at 1200°C. No simple relationship can explain the range of behaviors observed. Lifetime predictions based on 1000 hr (vertical dashed line) would fail to predict the behavior of most of these materials. For example, FeCrAl codoped with 0.1 at.%Y_2O_3 and 0.1 at.%Ta_2O_5 initially lost a significant amount of mass, but lasted as long as the alloy codoped with TiO_2. The best alloys require even longer times to begin spallation.

Spallation models tend to emphasize the accumulation of damage or defects, such as cracks in the scale which lead to spallation. It is commonly assumed that these defects result from thermal cycling. Lowell *et al.*[12,13] considered the effects of cycle duration on oxide spallation behavior in the development of an oxidation life-prediction model for superalloys in aircraft engine service. The model assumed that the loss of oxide occurred by spallation within the oxide scale (not to bare metal) in a random fashion over the alloy surface, with the fraction of scale lost in a given segment of the surface being described by one of several statistical distributions. Because the amount of oxide lost depended on the time available for scale growth between successive spallation events, the cycle dwell time was an important parameter. The model predicted that decreasing the cycle frequency would increase maximum mass change and decrease the number of cycles to net specimen mass loss. Their data for Ni–30Cr showed this effect when mass change vs. number of cycles was plotted for cycles from 5 to 300 min. However, when the data are replotted vs. time at temperature, cycles from 5 to

Table II. ized Life in 1-hr cycles at 1200°C for Various Fe-Base Alloys Extrapolated to a Uniform 1.5-mm Specimen Thickness[a].

Alloy	Actual thickness (mm)	Normalized life 1-hr cycles, 1200°C 1.5-mm thickness
Fe–28Al–2Cr (FAS)	1.0	2500
FAL (Zr)	1.0	3450
FAL (Zr)	1.3	3100
FAP (16Al, Zr)	0.9	1270
FAS + Hf	1.7	**9100**
PMFAS	1.5	3900
FeCrAl	1.5	310
FeCrAlY	1.5	**9050**
PM2000 (Y_2O_3)	1.7	3500
APM (ZrO_2)	1.2	5100
FeCrAl + Y_2O_3	1.4	1570
FeCrAl + Y_2O_3/CaO	1.5	3100
FeCrAl + Y_2O_3/MgO	1.5	1300
FeCrAl + Y_2O_3/Ta_2O_5	1.5	1650
FeCrAl + Y_2O_3/TiO_2	1.5	1700
FeCrAl + La_2O_3	1.4	2400
FeCrAl + HfO_2	1.5	2950
FeCrAl + SrO	1.5	3100
FeCrAl + Yb_2O_3	1.5	560

[a]Two specimens are still being tested.

60 min showed no difference in mass change, and only for 5-hr cycles was there less spallation. This is similar to the small effect observed in this study between 1- and 2-hr cycles, e.g., Figs. 5, 8, and 11.

Recent work has compared scales grown isothermally to those grown in 1-hr cycles to look for evidence of damage accumulation,[46,53] on NiCrAlY and NiAl + Hf oxidized for 100 hr at 1100°C, PMFAS oxidized 20 hr at 1200°C, and FeCrAlY oxidized 200 hr at 1200°C. In none of these cases was there significant difference between the isothermally and cyclicly grown oxide microstructures and no evidence of incipient damage. These results suggest that critical damage, which leads to scale spallation, is either very localized or that another mechanism is necessary to explain spallation. There was no indication that uniform small defects are formed in the scale as a result of thermal cycling.

The less frequently observed detrimental effect of decreasing cycle frequency (i.e., more spallation with longer time cycles) requires a different type of mechanism than what is described above by Lowell and others. There are processes that occur isothermally, such as oxidation-induced deformation of the substrate and growth of interfacial voids and dopant-rich oxides (such as, Ta-rich oxides on superalloys[19]), which may have different effects when the cycle frequency is changed. Allowing these defects

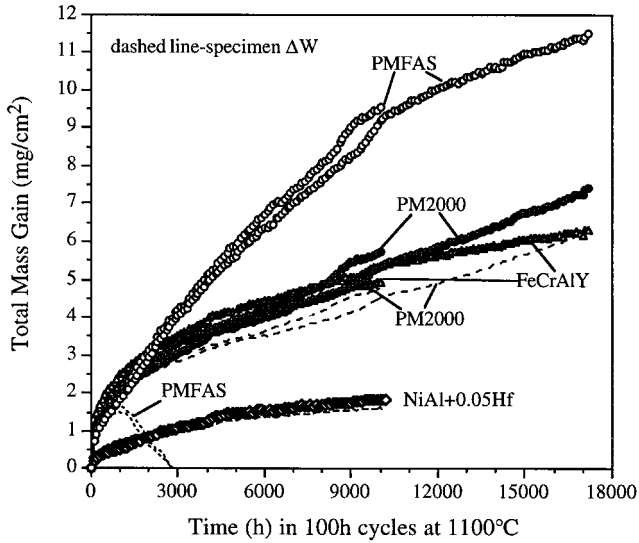

Fig. 16. Total and specimen (dashed lines) mass gains for several alumina-forming alloys in 100-hr cycles at 1100C. The scale on PMFAS spalls readily resulting in a high total mass gain. The slow-growing adherent scale on NiAl + Hf results in the lowest mass gains.

to increase in size (by increasing the length of the cycle) may change the spallation event from a localized minor event, such as that nucleated by a small defect, to a much larger event affecting a large fraction of the scale. Discussion of the specific mechanisms by which each type of material reacts to a change in the cycle frequency is beyond the scope of this paper. Future work in this area should include microstructure characterization work (which will be included in a subsequent paper[18]), and include time-series to show microstructure development.

The time at which the effect of cycle frequency begins to be observed appeared to be a strong function of substrate scale adhesion. For defect-free NiAl + Hf, that time exceeds 1000 hr at 1200°C, compared to about 500 hr for FeCrAlY, 100 hr for iron aluminides, and very short times for most undoped alumina formers (Figs. 4–13). This result is not surprising because, until the scale starts to spall, it grows at a rate essentially equal to that under isothermal conditions. This critical time is an important factor in terms of experimental design. Only by exceeding the critical time can the effect of cycle frequency be evaluated. For example, the effect of cycle frequency is not definitive for NiAl + Hf, because the experiments have not been run for a sufficiently long time and the casting quality issue complicates the data. On the other hand, once the time to significant spallation has been

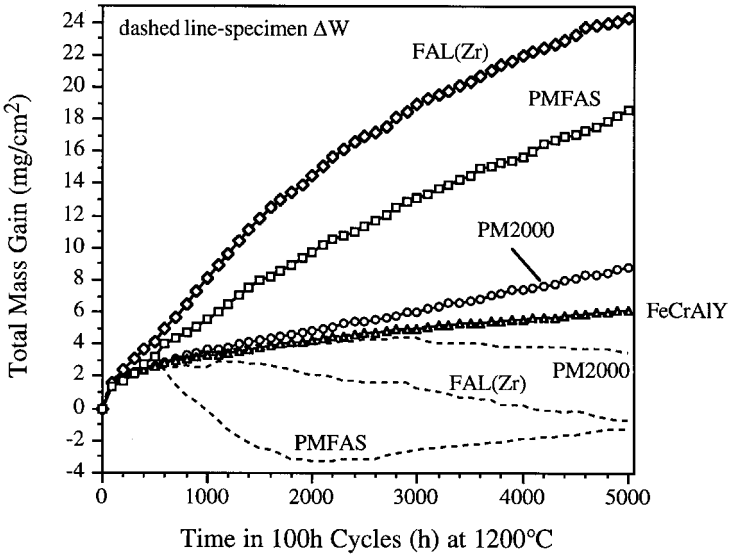

Fig. 17. Total and specimen mass gains for several Fe-base alloys in 100-hr cycles at 1200°C. Whereas there were various behaviors for the specimen mass change, the total mass gains were more well-behaved. The total mass gain is directly proportional to the metal wastage and, therefore, can be used to predict lifetime. No spallation was observed for FeCrAlY as the total and specimen mass gains coincided.

established, the scale can be examined before and after this critical time. For example, with Ni–20 wt.%Cr–10Al + Y in 1-hr cycles at 1100°C, because spallation, which became significant after 200 hr, makes specimen preparation difficult, it was necessary to examine the scale after 100 hr.[53]

The shape of the specimen mass-gain curve also is an important factor for modeling oxidation behavior. In general, the Ni-base alloys exhibit more regular behavior, with a protective period followed by a nearly linear mass-loss period as the alloy begins to spall (Figs. 1, 2, 5, and 6). This type of behavior has been successfully modeled by workers at the NASA Lewis Research Center[12–14,54–56] and others.[57] However, a linear mass loss was not as clearly observed in Fe-base alloys, which were not included in these previous modeling efforts. As illustrated in Fig. 14, the spallation curves often have a nearly zero rate loss period not typically observed in Ni-base alloys. Even this figure is an oversimplification, as there is a wide variety of behaviors, as shown in Fig. 15. This complication makes it difficult to apply models, such as those developed for Ni-base alloys, to Fe-base alloys. As suggested by the data in Figs. 16 and 17, it may be easier to model lifetime

if the total mass gain (obtained from a contained-cyclic test) is used, rather than only the specimen mass change. The total mass-gain curves are easily fitted to an exponential or other function to predict lifetimes.

These tests have sought to avoid the effect of specimen thickness on oxidation performance. However, it is an essential one for modeling. Ongoing work at ORNL will eventually supplement the limited data available here. Table II uses a linear extrapolation for lifetime and thickness.[52] For 1-hr cycles at 1200°C, this approximation was found to be more accurate than a higher exponent, but it has not been sufficiently verified. Other work in this area,[58] including the use of different specimen geometries,[59] has been recently reported. Obviously this is a critical issue for the development of oxidation lifetime models.

Thus, an important underlying issue on the effect of cycle frequency concerns the method by which the oxidation test is conducted. There are two general methods, uncontained and contained testing; both have strengths and weaknesses, depending on the goals of the test.

Uncontained Testing

This type of experiment is characterized by specimens hanging in a furnace, but not contained in a crucible, and is more widely used in oxidation experiments. One of the benefits of this type of test is that it is more flexible and easier to conduct. This method is also preferred for complex environments, such as mixed gas or water vapor, where it is necessary to ensure that the specimen experiences a constant gas composition or where gas velocity may be a variable. With a computer-controlled, cyclic-testing rig, essentially any cycle time can be used and cooling can be easily modified by the rate of withdrawal or by using forced gas cooling upon removal from the furnace. In any case, heating and cooling times are relatively short. However, one of the important failings of this type of test is that it does not measure the total mass gain; when the specimen scale spalls, only the specimen mass change can be accurately measured. This is less of a problem for Ni-base alloys, which are more well-behaved than Fe-base alloys.

Sources of error for mass-change measurements in uncontained testing are the evaporation of the Pt–Rh wire, which runs through a hole in the specimen (for a 2-cm long, 0.5-mm diameter wire this can vary from 0.4 μg/hr at 1000°C to 12 μg/hr at 1200°C in flowing O_2) and the uncertainty regarding chromia volatilization vs. spallation for mass losses of chromia formers.[17] Depending on the friability of the scale, there may also be more or less scale lost from the specimen, depending on how it is handled, particularly while being weighed.

Contained Testing

This type of test is characterized by placing a specimen in an individual crucible, with a lid, to contain any spalled or volatile oxidation products. Since the crucible and contents are weighed at each interval, the primary benefit of this test is that it yields the total mass gain (including spallation products) and appears to retain most evaporated species on the crucible walls and lid.[17] This allows better assessments of relative metal consumption rates than are possible from the specimen mass change alone. The spalled or evaporated mass is directly quantified without any experimental assumptions and is available for chemical analysis. However, because of possible violent or "energetic" spallation, thermal drafts and/or volatilization, the validity of this test is far more questionable if a crucible lid is not used.

However, there are several limitations of contained testing. Because of the large thermal mass and problem of thermal shock of alumina, short cycles are impractical. Also, when a set of multiple crucibles are inserted into a preheated tube furnace, the furnace temperature is often altered for 10 min or more. For 1- or 2-hr cycles this would cause a significant difference in the thermal history of the specimen compared to uncontained tests or longer cycles. This test is best suited for 10-hr or longer cycles to avoid such problems. Furthermore, because the specimen is isolated in a crucible, it is difficult to use environments other than air. With increased emphasis on the effect of mixed-gas environments and, particularly, water vapor in combustion environments,[60,61] this is a significant limitation. For iron aluminides, which can exhibit accelerated oxidation in air compared to O_2,[22,62] this is also a concern. Another drawback is that weighing the crucible, the specimen, and then the crucible without the specimen (as a check) is much more time consuming than merely weighing the specimen. Specimen size also is restricted by the size of the crucible.

The sources of error in contained testing are more varied. One factor is that an alumina crucible mass (10–13 g) is often an order of magnitude larger than that of the specimen (1–2 g). For low specimen mass gains, slight changes in the crucible mass can distort the total mass gain.[17] This problem can be corrected in a similar manner to the evaporation of Pt and is most strongly encountered after the first cycle. For well-used crucibles, mass changes (mainly slight losses) are typically 0.1 mg per 1000 hr of usage. In general, for mass changes like those observed at 1200°C (Fig. 17), this error is extremely small.

As initially mentioned, the issue of cycle frequency is rarely discussed in the open literature although it is an extremely important variable. In terms of approximating the expected service conditions and developing accurate lifetime models, it is essential to fully understand this issue and

considerably more work in this area is needed. It is hoped that additional work will be pursued on this general topic that will more fully explore some of the issues not examined here.

SUMMARY

The issue of cycle frequency in oxidation testing is far from resolved, but a number of important points can be emphasized. First, the effect of cycle frequency is not uniform among different alloy classes. It is highly dependent on the scale adherence to the substrate, the total test time, and (likely) the test temperature. Cycle frequency also affects how the test should be performed, as longer-term cycles (100 hr) are better suited for contained testing in alumina crucibles and shorter cycles (1–2 hr) require uncontained testing. In general, the objectives of the testing strongly influence the test procedures. For life prediction, total mass gain from contained testing is very valuable and reliable, particularly for Fe-base alloys, which perform somewhat differently than Ni-base alloys. Further work will be required to fully understand the issue of cycle frequency and its implications on high-temperature oxidation performance.

ACKNOWLEDGMENTS

The authors are indebted to M. J. Bennett (formerly of Harwell Laboratory, U.K.) who started us on our program on contained cyclic testing. The authors also would like to thank M. Howell, L. D. Chitwood, G. Garner, N. Bonwit, and C. Roberts at ORNL for many hours of assistance with the experimental work and J. R. DiStefano and J. A. Haynes at ORNL for their comments on the manuscript. This research was sponsored by the U.S. Department of Energy, Fossil Energy Advanced Research and Technology Development Materials Program and the Advanced Turbine Systems program under contract DE-AC05-00OR22725 with UT-Battelle, LLC.

REFERENCES

1. C. A. Barrett and E. B. Evans, *Am. Ceram. Soc. Bull.* **52**, 353 (1973).
2. C. E. Lowell and D. L. Deadmore, *Oxid. Met.* **14**, 325 (1980).
3. R. Mevrel, *Mater. Sci. Technol.* **3**, 531 (1987).
4. M. Schütze, *Protective Oxides Scales and Their Breakdown* (Wiley, Chichester, U.K., 1997).
5. H. Jonas and J. A. Golczewski, *J. Nucl. Mater.* **120**, 272 (1984).
6. H. E. Evans, *Mater. Sci. Technol.* **4**, 415 (1988).
7. P. Hancock and J. R. Nicholls, *Mater. Sci. Technol.* **4**, 398 (1988).
8. M. J. Bennett, H. E. Evans, and D. A. Shores, *Mater. High Temp.* **12**, 127 (1994).
9. J. Jedlinski, M. J. Bennett, and H. E. Evans, *Mater. High Temp.* **12**, 169 (1994).
10. H. E. Evans, J. R. Nicholls, and S. R. J. Saunders, *Solid State Phenomenon* **41**, 137 (1995).

11. J. R. Nicholls, H. E. Evans, and S. R. J. Saunders, *Mater. High Temp.* **14**, 5 (1997).
12. C. E. Lowell, S. R. Levine, and S. J. Grisaffe, in *Proc. 1974 Gas Turbine Materials in the Marine Environment Conference*, MCIC Rep. No. 75-27 (Metals and Ceramics Information Center, Battelle, Columbus, OH, 1975), pp. 535–554.
13. C. E. Lowell, J. M. Smialek, and C. A. Barrett, in *High-Temperature Corrosion*, R. A. Rapp, ed. (NACE, Houston, TX, 1983), pp. 219–226.
14. J. L. Smialek, J. A Nesbitt, C. A. Barrett, and C. E. Lowell, in *Cyclic Oxidation of High Temperature Materials*, M. Schütze and W. J. Quadakkers, eds. (Institute of Materials, London, U.K., 1999), pp. 148–168.
15. "Comprehensive Program Plan for Advanced Turbine Systems," Office of Fossil Energy and Office of Energy Efficiency and Renewable Energy, Department of Energy, Report to Congress No. DOE/FE-0279, July 1993.
16. W. P. Parks, E. E. Hoffman, W. Y. Lee, and I. G. Wright, *J. Thermal Spray* **6**, 187 (1997).
17. B. A. Pint, P. F. Tortorelli, and I. G. Wright, in *Cyclic Oxidation of High Temperature Materials*, M. Schütze and W. J. Quadakkers, eds. (Institute of Materials, London, U.K., 1999), pp. 111–132.
18. B. A. Pint and I. G. Wright, manuscript in progress.
19. I. G. Wright, B. A. Pint, W. Y. Lee, K. B. Alexander, and K. Prüßner, in *High Temperature Surface Engineering*, J. Nicholls and D. Rickerby, eds. (Institute of Materials, London, U.K., 1999), pp. 95–113.
20. B. A. Pint, *Oxid. Met.* **49**, 531 (1998).
21. B. A. Pint, I. G. Wright, W. Y. Lee, Y. Zhang, K. Prüßner, and K. B. Alexander, *Mater. Sci. Eng.* **A245**, 201 (1998).
22. B. A. Pint, P. F. Tortorelli, and I. G. Wright, *Mater. High Temp.* **16**, 1 (1999).
23. B. A. Pint, K. L. More, P. F. Tortorelli, W. D. Porter, and I. G. Wright, *Mater. Sci. Forum* **369–372**, 411 (2001).
24. B. A. Pint, *Mater. Sci. Forum* **251–254**, 397 (1997).
25. B. A. Pint and K. B. Alexander, *J. Electrochem. Soc.* **145**, 1819 (1998).
26. I. G. Wright, B. A. Pint, and P. F. Tortorelli, *Oxid. Met.* **55**, 333 (2001).
27. B. A. Pint, P. F. Tortorelli, and I. G. Wright, *Mater. Corros.* **47**, 663 (1996).
28. A. W. Funkenbush, J. G. Smeggil, and N. S. Bornstein, *Metall. Trans.* **16A**, 1164 (1985).
29. J. L. Smialek, D. T. Jayne, J. C. Schaeffer, and W. H. Murphy, *Thin Solid Films* **253**, 285 (1994).
30. J. L. Smialek and B. K. Tubbs, *Metall. Trans.* **26A**, 427 (1995).
31. G. H. Meier, F. S. Pettit, and J. L. Smialek, *Werkst. Korros.* **46**, 232 (1995).
32. M. A. Smith, W. E. Frazier, and B. A. Pregger, *Mater. Sci. Eng.* **A203**, 388 (1995).
33. C. Sarioglu, C. Stinner, J. R. Blachere, N. Birks, F. S. Pettit, and G. H. Meier, in *Superalloys 1996*, R. D. Kissinger, D. J. Deye, D. L. Anton, A. D. Cetel, M. V. Nathal, T. M. Pollack, and D. A. Woodford, eds. (TMS, Warrendale, PA, 1996), pp. 71–80.
34. K. Prüßner and I. G. Wright, unpublished research, Oak Ridge National Laboratory, Oak Ridge, TN, 1998 (in Fig. 3).
35. D. P. Moon, *Mater. Sci. Technol.* **5**, 754 (1989).
36. A. Strawbridge and P. Y. Hou, *Mater. High Temp.* **12**, 177 (1994).
37. B. A. Pint, *Oxid. Met.* **45**, 1 (1996).
38. I. G. Wright and B. A. Pint, in *Proc. SF2M 2000, Journées d'automne (Société Française de Métallurgie et de Matériaux, Paris, 2000)*, p. 86.
39. E. C. Dickey, B. A. Pint, K. B. Alexander, and I. G. Wright, *J. Mater. Res.* **14**, 4531 (1999).
40. B. M. Warnes and D.C. Punola, *Surf. Coating Technol.* **94–95**, 1 (1997).
41. Y. Zhang, W. Y. Lee, J. A. Haynes, I. G. Wright, B. A. Pint, K. M. Cooley, and P. K. Liaw, *Mater. Trans.* **30A**, 2679 (1999).
42. J. L. Smialek, *Metall. Trans.* **9A**, 309 (1978).
43. B. A. Pint, *Oxid. Met.* **48**, 303 (1997).
44. C. S. Wukusick and J. F. Collins, *Mater. Res. Std.* **4**, 6376 (1964).
45. F. A. Golightly, F. H. Stott, and G. C. Wood, *J. Electrochem. Soc.* **126**, 1035 (1979).

46. P. F. Tortorelli, B. A. Pint, E. Kenik, K. L. More, and I. G. Wright, *Mater. Sci. Forum* **369–372**, 337 (2001).
47. B. A. Pint, P. F. Tortorelli, and I. G. Wright, ORNL Report to be published 2002, Oak Ridge, TN.
48. F. H. Stott, F. A. Golightly, and G. C. Wood, *Corros. Sci.* **19**, 889 (1979).
49. W. J. Quadakkers and M. J. Bennett, *Mater. Sci. Technol.* **10**, 126 (1994).
50. W. J. Quadakkers and K. Bongartz, *Werkst. Korros.* **45**, 232 (1994).
51. I. G. Wright, B. A. Pint, C. S. Simpson, and P. F. Tortorelli, *Mater. Sci. Forum* **251–254**, 195 (1997).
52. I. G. Wright, B. A. Pint, L. M. Hall, and P. F. Tortorelli, eds., in *Proc. EFC Workshop on Lifetime Modeling*, Frankfurt, Germany, February 2001, in press.
53. B. A. Pint, K. L. More, I. G. Wright, and P. F. Tortorelli, *Mater. High Temp.* **17**, 165 (2000).
54. J. A. Nesbitt, *J. Electrochem. Soc.* **136**, 1511–1517 and 1518–1527 (1989).
55. C. E. Lowell, C. A. Barrett, R. W., Palmer, J. V. Auping, and H. B. Probst, *Oxid. Met.* **36**, 81 (1991).
56. J. A. Nesbitt, E. J. Vinarcik, C. A. Barrett, and J. Doychak, *Mater. Sci. Eng.* **A153**, 561 (1992).
57. K. S. Chan, N. S. Cheruvu, and G. R. Levant, ASME 97-GT–389, presented at the International Gas Turbine & Aeroengine Congress & Exhibition, Orlando, FL, June, 1997.
58. J. P. Wilber, M. J. Bennett, and J. R. Nicholls, *Mater. High Temp.* **17**, 125 (2000).
59. G. Tatlock and H. Al Badairy, *Oxid. Met.* **53**, 157 (2000).
60. H. Nickel, Y. Wouters, M. Thiele, and W. J. Quadakkers, *Fresenius' J. Anal. Chem.* **361**, 540 (1998).
61. B. A. Pint and J. M. Rakowski, NACE Paper 00–259, Houston, TX, 2000.
62. B. A. Pint, J. Regina, K. Prüßner, L. D. Chitwood, K. B. Alexander, and P. F. Tortorelli, *Intermetallics* **9**, 735 (2001).